Title

Proximate controls on semiarid soil greenhouse gas fluxes across 3 million years of soil development

Journal

Biogeochemistry, 125(3)

ISSN

0168-2563

Authors

Sullivan, BW
Nasto, MK
Hart, SC
et al.

Publication Date

2015-09-01

DOI

10.1007/s10533-015-0133-0

Peer reviewed

Biogeochemistry (2015) 125:375–391
DOI 10.1007/s10533-015-0133-0

Proximate controls on semiarid soil greenhouse gas fluxes across 3 million years of soil development

Benjamin W. Sullivan · Megan K. Nasto · Stephen C. Hart ·
Bruce A. Hungate

Received: 31 January 2015 / Accepted: 11 August 2015 / Published online: 25 August 2015

Abstract Soils are important sources and sinks of three greenhouse gases (GHGs): carbon dioxide (CO_2), methane (CH_4), and nitrous oxide (N_2O). However, it is unknown whether semiarid landscapes are important contributors to global fluxes of these gases, partly because our mechanistic understanding of soil GHG fluxes is largely derived from more humid ecosystems. We designed this study with the objective of identifying the important soil physical and biogeochemical controls on soil GHG fluxes in semiarid soils by observing seasonal changes in soil GHG fluxes across a three million year substrate age gradient in northern Arizona. We also manipulated soil nitrogen (N) and phosphorus availability with 7 years of fertilization and used regression tree analysis to identify drivers of unfertilized and fertilized soil GHG fluxes. Similar to humid ecosystems, soil N_2O flux was correlated with changes in N and water availability and soil CO_2 efflux was correlated with changes in water availability and temperature. Soil CH_4 uptake was greatest in relatively colder and wetter soils. While fertilization had few direct effects on soil CH_4 flux, soil nitrate was an important predictor of soil CH_4 uptake in unfertilized soils and soil ammonium was an important predictor of soil CH_4 uptake in fertilized soil. Like in humid ecosystems, N gas loss via nitrification or denitrification appears to increase with increases in N and water availability during ecosystem development. Our results suggest that, with some exceptions, the drivers of soil GHG fluxes in semiarid ecosystems are often similar to those observed in more humid ecosystems.

Keywords Carbon dioxide · Methane · Nitrous oxide · Nutrient addition · Seasonality · Substrate age gradient

Introduction

Carbon dioxide (CO_2), methane (CH_4), and nitrous oxide (N_2O) are important greenhouse gases (GHGs) exchanged between soils and the atmosphere.

Responsible Editor: Marc Kramer.

B. W. Sullivan (✉)
Department of Natural Resources and Environmental Science, University of Nevada-Reno, 1664 N Virginia Street, Mail Stop 186, Reno, NV 89557, USA
e-mail: bsullivan@cabnr.unr.edu

M. K. Nasto
College of Forestry and Conservation, University of Montana, 32 Campus Drive, Missoula, MT 59812, USA

S. C. Hart
Life and Environmental Sciences and Sierra Nevada Research Institute, University of California, Merced, 5200 N. Lake Road, Merced, CA 95343, USA

B. A. Hungate
Department of Biological Sciences and Center for Ecosystem Science and Society, Northern Arizona University, Flagstaff, AZ 86011, USA

Combined, all three GHGs constitute almost 90 % of the total radiative forcing from long-lived GHGs in the atmosphere (Houghton et al. 1996; Shine and Sturges 2007; Montzka et al. 2011), and N_2O contributes to stratospheric ozone depletion (Crutzen 1974). The atmospheric concentrations of CO_2, CH_4, and N_2O have risen sharply since the pre-industrial era, likely as a result of land use change, fossil fuel consumption, and large-scale animal husbandry (Ciais et al. 2013).

Well-drained (aerobic) soils are important sources and sinks of CO_2, CH_4, and N_2O. The production of CO_2 in soil by plant root and microbial respiration is one of the largest carbon (C) fluxes globally (Hashimoto et al. 2015). The oxidation of atmospheric CH_4 by methanotrophic bacteria in aerobic soil is the only known terrestrial sink of atmospheric CH_4 (Le Mer and Roger 2001). However, anaerobic soil conditions cause net soil CH_4 production (Segers 1998). Given sufficient N availability, soil may either produce N_2O as a byproduct of nitrification (an aerobic process) and denitrification (an anaerobic process; Webster and Hopkins 1996; Bremner 1997), or consume N_2O when the reduction of N_2O to dinitrogen gas (N_2) exceeds N_2O production (Chapuis-Lardy et al. 2007).

Despite the significance of these gases to the global energy balance, rates of soil GHG fluxes and the proximate mechanisms that control soil GHG fluxes are unclear in many terrestrial ecosystems. This is especially true in arid and semiarid ecosystems that are generally understudied relative to their land area (Martin et al. 2012). For example, in a global inventory of studies that measured soil CH_4 uptake, only five out of a total 318 studies occurred in hot or cold deserts, and three more in ecosystems classified as chaparral (Dutaur and Verchot 2007). In total, these eight studies accounted for ecosystems that cover ~40 % of the Earth's land surface, provide food and shelter to 41 % of the human population, and store 27 % of the global C stock (Reynolds 2001; Lal 2004; Safriel and Adeel 2008).

Soil temperature, nitrogen (N), phosphorus (P), and water are often broadly described as first-order controls on plant- and microbial-mediated processes like soil GHG fluxes (Vitousek and Howarth 1991; Running et al. 2004; Elser et al. 2007; Mahecha et al. 2010). In unfrozen soil, soil CO_2 efflux is a function of the availability of C sources (driven by gross primary productivity; Raich and Schlesinger 1992), sufficient available N and P (Neff et al. 2002; Cleveland and Townsend 2006), warm temperatures (e.g., Q_{10} functions; Mahecha et al. 2010), and increasing water availability (provided soils stay aerobic; Orchard and Cook 1983; Raich and Schlesinger 1992). Soil CH_4 uptake has been modeled strictly as a function of soil texture and soil water content (Potter et al. 1996; Striegl 1993) based on evidence that methanotrophic bacteria are chiefly limited by the supply of CH_4 and oxygen (O_2) into soil (which requires abundant soil air-filled pore space) and water (which limits gaseous diffusion and cellular activity). Soil N_2O production is often attributed to denitrification, which requires sufficient soil water content for anaerobic conditions, sufficient N availability for nitrate (NO_3^-) production, and an energy source like dissolved organic carbon (DOC; Nömmik 1956). On the other hand, soil N_2O production can also result from nitrification, an aerobic process that is typically highest at intermediate soil water contents (Stark and Firestone 1995), and soil N_2O consumption can occur when N availability is low (Chapuis-Lardy et al. 2007).

Most of the relationships between temperature, soil water availability, soil nutrient availability, and soil GHG fluxes were identified in humid climates. However, these relationships may not hold for more xeric climates because these ecosystems often have different biogeochemistry and limitations than more mesic ecosystems (Austin et al. 2004; Austin 2011), with unexpected and counter-intuitive consequences. For example, in six of seven terrestrial biomes, litter decomposition (an important source of soil CO_2 efflux) was predicted by litter quality and climatic conditions. In arid grasslands, however, these variables failed to predict litter decomposition rates due to the effects of photo-oxidation (Parton et al. 2007). High rates of soil CH_4 uptake have been repeatedly measured in dry environments with soil water contents less than one percent, by mass (Striegl et al. 1992; Galbally et al. 2010; Sullivan et al. 2013)—a result attributed to the adaptation of specialized methanotrophic bacteria to arid soils. Furthermore, available N pools and transformations, such as nitrification (a means of soil N_2O production), may be significantly greater during dry seasons than wet seasons (Parker and Schimel 2011; Sullivan et al. 2012). Such results, and a perhaps misplaced emphasis on water as a limiting factor in arid soils (Austin 2011), cast doubt on the applicability of the aforementioned mechanisms controlling GHG fluxes in arid soils.

Here, we assessed how soil CO_2, CH_4, and N_2O fluxes changed as a function of soil fertility and the soil physical environment along the three million year Substrate Age Gradient of Arizona (SAGA). The SAGA is well suited to elucidate proximate controls on GHG fluxes in semiarid ecosystems because it has strong, naturally occurring gradients of soil texture, water holding capacity, and soil C, N, and P (Table 1; Selmants and Hart 2008, 2010), in addition to substantial seasonal climatic variability (Sheppard et al. 2002). Further, the three oldest SAGA sites experienced seven years of fertilization with N, P, and N and P in combination (N + P) prior to our study, allowing for experimental evaluation of the relationships between soil GHG fluxes and soil nutrient availability. Importantly for this project, the SAGA has repeatedly shown soil C and N patterns consistent with ecosystem retrogression (Selmants and Hart 2008; Sullivan et al. 2012), a unimodal pattern of C and N pools and fluxes that has been attributed to reduced P availability during soil genesis (Selmants and Hart 2008; Peltzer et al. 2010). Similarly, Selmants and Hart (2008) found increasing rates of fractionating soil nitrogen transfomations, such as nitrification and denitrification, and a corresponding increase in soil and plant ^{15}N isotope signatures, all of which indicate greater N availability with substrate age. Finally, after 1 year of N and P fertilization among these sites, N fertilization increased grass primary production on younger land surfaces and P fertilization increased grass primary production on older land surfaces (Newman and Hart 2015).

Methods

Study sites

This study was conducted on the SAGA within the San Francisco Volcanic Field (SFVF) in a woodland ecosystem. The entire SFVF is ~5000 km^2 in size (Priest et al. 2001) and is located along the southern margin of the Colorado Plateau in central-northern Arizona, USA. Since its formation during the Pliocene Epoch, volcanic activity has migrated in an east-northeast direction at a rate of ~2 cm per year due to the North American Plate moving over a stationary magmatic hot spot (Tanaka et al. 1986). The volcanism resulted in over 600 monogenetic basaltic cinder

Table 1 Substrate age, location, elevation, mean annual precipitation (MAP), mean annual temperature (MAT), % clay content, field capacity, soil total carbon (C) to nitrogen (N) ratio, total C, total N, total (Kjeldahl) phosphorus (P), and tree basal area along the Substrate Age Gradient of Arizona (SAGA)

Substrate age (ky)	Location (Lat., Long.)	Elevation (m)	MAP (mm)[a]	MAT (°C)[a]	Clay[b] (%)	Total C:N[b]	Total C (g kg^{-1})[b]	Total N (g kg^{-1})[b]	Total P (g m^{-2})[c]	Tree basal area (m^2 ha^{-1})[d]
0.93	35.394°N, 111.424°W	1905	328 (42)	12 (0.2)	1.13	18.4	2.8	0.2	375	5.7
55	35.246°N, 111.458°W	1941	352 (39)	11 (0.3)	8.38	11.6	9.4	0.9	250	11.6
750	35.538°N, 111.867°W	2073	325 (42)	11 (0.2)	31.84	13.9	23.2	1.9	165	20.7
3000	35.391°N, 112.141°W	2003	338 (40)	11 (0.2)	37.15	12.5	13.1	1.2	150	18.3

[a] Mean with standard error in parentheses, 2002–2005, Selmants (2007)

[b] Selmants and Hart (2008)

[c] Selmants and Hart (2010)

[d] Live plus recently dead piñon and juniper, Looney et al. (2012)

cone volcanoes ranging in age from ~6,000,000 to <1000 years (Tanaka et al. 1986).

The SAGA is comprised of four sites within the extent of the SFVF. The substrate ages of these sites are approximately 0.93, 55, 750, and 3000 ky, yet other soil forming factors such as current climate, topography, vegetation, and parent material are constant (sensu lato, Jenny 1941; Selmants and Hart 2008). The sites were aged using dendrochronology and archaeology at the 0.93 ky site and potassium argon dating at the three older sites (Selmants and Hart 2008). The underlying substrate is a pyroclastic sheet of volcanic cinders, consisting primarily of microporphyritic basalt (Moore and Wolfe 1987). Relatively flat topography (<1 % slope) and stable landscape positions allow for in situ weathering of the basalt parent material (Selmants and Hart 2008) and an increase in the soil fine-textured fraction with increasing substrate age. Mean annual air temperature of the SAGA sites is ~11 °C and mean annual precipitation is ~340 mm (Selmants and Hart 2008); air temperatures in the region can range between 37 and −33 °C (1981–2010 data from nearby Sunset Crater National Monument (SCNM) weather station; ncdc.noaa.gov). Annual precipitation ranged between 236 and 660 mm across thirty years (1981–2010; SCNM weather station). Seasonal precipitation dynamics cause roughly half the annual precipitation to fall as snow between December and March, and the other half to fall as rain during monsoonal thunderstorms between July and September (Sheppard et al. 2002). The four sites are open piñon pine (*Pinus edulis* Engelm.) and one-seed juniper (*Juniperus monosperma* Engelm.) woodlands. Blue gramma grass (*Bouteloua gracilis* (Wild. Ex Dunth) Lag. Ex Griffiths), a C_4 perennial grass, dominates the inter-tree canopy vegetation of the three oldest sites, while woody shrubs (*Rhus trilobata* Nutt., *Fallugia paradoxical* (D. Don) Endl., *Ephedra viridi* Coville) are present in inter-canopy spaces at the youngest site.

Nutrient availability varies among the SAGA sites in a manner consistent with biogeochemical theory (Walker and Syers 1976; Vitousek and Farrington 1997). Pools and fluxes of atmospherically derived nutrients (e.g., C and N) increased with substrate age to a maximum and then declined (Selmants and Hart 2008) during ecosystem retrogression (Peltzer et al. 2010). Retrogression has been attributed to the steady decline in P availability as a function of increasing substrate age (Selmants and Hart 2010).

Nitrogen, P, and N + P were applied annually in *B. gracilis*-dominated intercanopy spaces of the three older sites (55, 750, and 3000 ky) between 2004 and 2010. In this experiment, the youngest site did not receive nutrient additions because of the relative scarcity of *B. gracilis*. The fertilization methodology is described in detail by Newman and Hart (2015). Nitrogen was applied as ammonium nitrate at a rate of 7.5 g N m^{-2} y^{-1} to the N and N + P plots; P was applied as a triple super phosphate at a rate of 5 g P m^{-2} y^{-1} to the P and N + P plots. Ten g N m^{-2} y^{-1} induced piñon tree mortality in a semiarid ecosystem in New Mexico, USA, so the N addition here was designed to minimize potential mortality while maximizing N inputs (Newman and Hart 2015). Phosphorus addition exceeded the sorption capacity of the soil and biological N:P requirements (Newman and Hart 2015). Nutrients were added by hand as pre-weighed granulated solids to the soil surface shortly before the onset of summer monsoonal rains (early July) each year. The timing of this addition was intended to increase the likelihood that the nutrients would be incorporated into the soil by the first monsoonal rains. A 1 m boundary separated each 1.5 m^2 plot from other plots, and each plot was trenched to 0.5 m mineral soil depth with a tile spade every year before fertilizer was applied. Nutrient additions were made to the 1.5 m^2 plots in a randomized complete block design with 8 blocks per site, from which we randomly selected 5 for GHG flux measurement. Blocks were fenced with barbed wire to minimize grazing by ungulates and free-range cattle. One plot in each of the five blocks was unamended and served as a control. We used these long-term fertilization plots to evaluate experimentally if nutrient availability limited the soil fluxes of CO_2, CH_4, and N_2O along the SAGA (see below).

Static chamber measures of GHGs

We measured CO_2, CH_4, and N_2O fluxes between the soil and atmosphere during days representative of the distinct conditions of the growing season of northern Arizona: the cool and wet post-snowmelt spring season, the warm and dry summer season, the warm and wet summer monsoon season, and the cool and dry fall season. We measured GHG fluxes in the middle of each distinct season: March 30th, June 1st, August 1st, and October 1st, 2010. The August 1st sampling point occurred approximately 25 days after fertilization at each of the three oldest sites. We used this temporal sampling design for the purpose of capturing seasonal dynamics in soil gas fluxes during each season, and correlating these fluxes with soil physical and chemical properties measured at that time. It was not our intention to scale these values to estimate annual fluxes, given the potential for errors in extrapolating the temporally limited dataset.

At the unfertilized 0.93 ky site, we randomly selected five plots from the eight intercanopy plots utilized by Selmants and Hart (2008). At the three older substrate ages, we randomly selected five of the eight fertilization treatment blocks described above. To measure soil GHG fluxes, we inserted one 30 cm diameter polyvinylchloride (PVC) collar 2 cm into the mineral soil in the center of the 1.5 m^2 plots. In March, we placed the collars in the soil several days before we sampled to minimize soil disturbance. The collars remained in the soil for the duration of the growing season. During each measurement period, we placed a 30 cm diameter PVC vented static chamber over the collar and sealed the chamber to the collar using a butyl rubber gasket. We measured changes in gas concentration over time by sampling chamber headspace gas 0, 15, 30, and 45 min after chamber installation with evacuated Silonite Minicans (Entech Instruments, Simi Valley, CA, USA). Each 100 mL Minican was over-pressurized to 160 mL. To reduce the effect of diel variability, we collected gas samples between the hours of 10:00 and 15:00 h local time during each measurement period. We quantified GHG concentrations from the headspace samples with an Agilent 6890 gas chromatograph equipped with a methanizer (Agilent Technologies, Palo Alto, CA, USA) that used a Haysep Q 60/80 column and a Porapak Q 60/80 column; both CO_2 and CH_4 concentrations were measured using a flame-ionization detector, while N_2O concentrations were measured using an electron capture detector. We calculated fluxes using a linear regression of CO_2, CH_4, and N_2O concentrations against the sampling interval and verified the linearity of the fluxes using the coefficient of determination. When an individual gas concentration measurement reduced the coefficient of determination below 0.50, we eliminated that concentration and calculated the flux based on three data points.

Soil physical environment

We used a soil thermometer (VWR Scientific, Inc., West Chester, PA, USA) to measure temperature at a 10 cm depth within a 0.5 m radius of the chamber collars inside each plot. Within the same radius, we also measured soil gravimetric water content (GWC) in the top 10 cm of mineral soil by collecting samples with a soil sampling tube (Oakfield Apparatus, Fon du Lac, WI, USA). Immediately after transport to the laboratory, a subsample was weighed, dried in an oven at 105 °C until it had reached a stable mass, and reweighed. We calculated the soil water potential (WP) of each sample using site-specific soil water release curves and our measurements of GWC. The water release curves were developed using a WP4 Dewpoint Potentiameter (Decagon Devices, Pullman, WA, USA), which measured soil WP at known GWCs.

Soil nutrient availability

At each sampling period, we measured available pools of N and P in the same top 10 cm of mineral soil used to measure WP and GWC from each plot where we measured GHG fluxes. We measured soil ammonium (NH_4^+) and NO_3^- concentrations by extracting 10 g of field moist soil with 50 mL of 2 M KCl, shaking for 1 h on a mechanical reciprocating shaker, and filtering through a Whatman no. 1 filter paper pre-leached with deionized water. Available N was assumed equivalent to total inorganic N ($NH_4^+ + NO_3^-$) concentrations. We estimated the soil available P pool as labile orthophosphate (PO_4^{3-}) using anion exchange membrane (AEM) strips. Approximately 1 g of field moist soil was placed in a 50 mL centrifuge tube with two AEM strips (10 × 50 mm; Ionic, Inc., Watertown, MA, USA) and 30 mL of deionized water, and the solution was rotated on an overhead shaker for 16 h at 30 rpm. We then removed and rinsed the AEM strips with deionized water, placed them in a clean 50 mL centrifuge tube, added 20 mL of 0.5 M HCl, and rotated the solution on an overhead shaker for 16 h. We froze the extracts for later analysis of NH_4^+, NO_3^-, and PO_4^{3-} concentrations using a QuickChem 8000 Flow Injection Autoanalyzer (Lachat Instruments, Loveland, CO, USA).

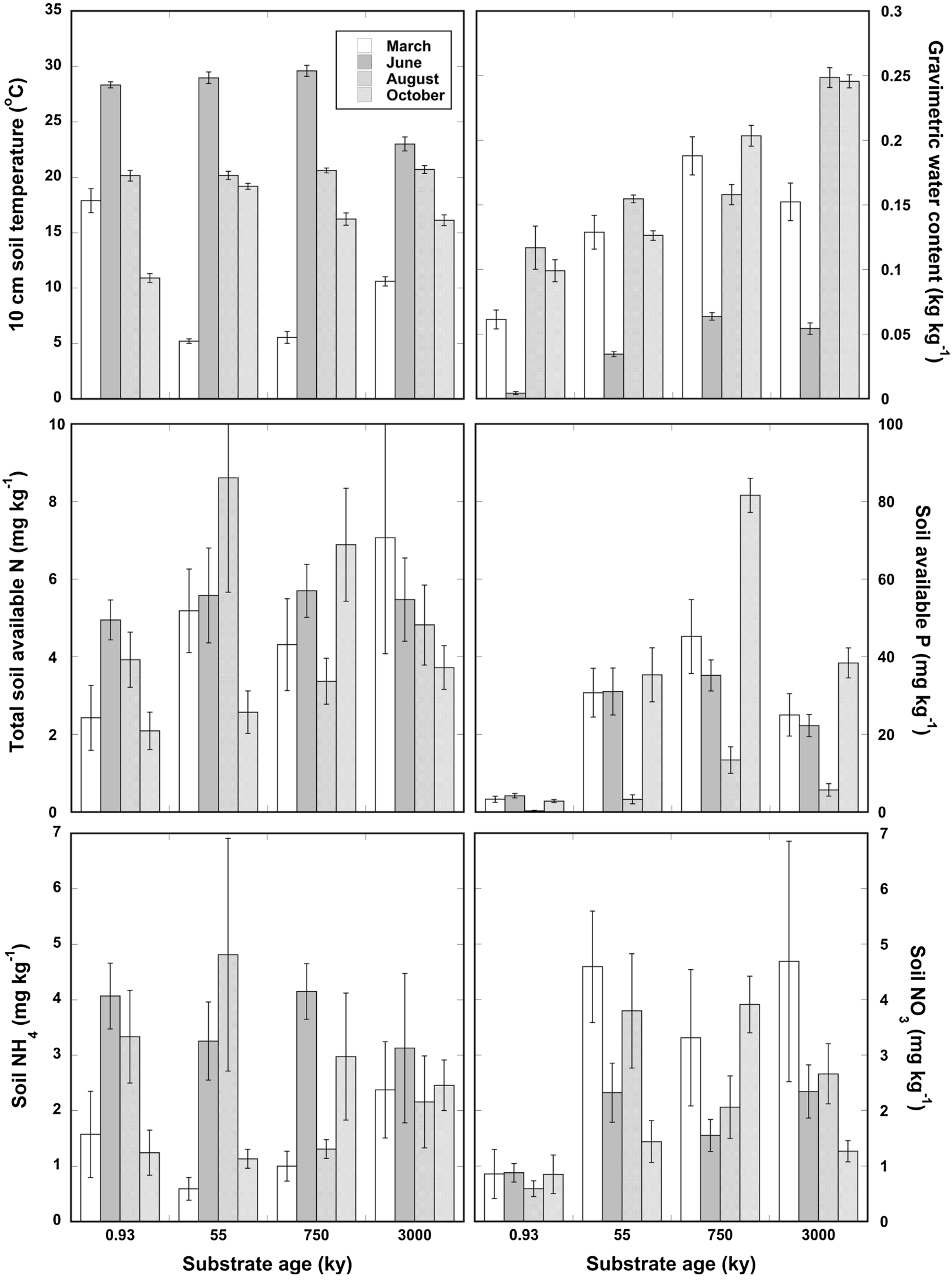
March
June
August
October
10 cm soil temperature (°C)
Gravimetric water content (kg kg-1)
Total soil available N (mg kg-1)
Soil available P (mg kg-1)
Soil NH4 (mg kg-1)
Soil NO3 (mg kg-1)
0.93
55
750
3000
Substrate age (ky)
35
30
25
20
15
10
5
0
0.3
0.25
0.2
0.15
0.1
0.05
10
8
6
4
2
100
80
60
40
20
7
6
5
4
3
2
1

◀**Fig. 1** Soil temperature (*top left panel*), gravimetric water content (*top right panel*), available nitrogen (N; sum of ammonium (NH_4^+) and nitrate (NO_3^-); *center left panel*), available phosphorus (P; resin-extractable orthophosphate; *center right panel*), soil NH_4^+ concentration (*bottom left panel*), and soil NO_3^- concentration (*bottom right panel*) measured during four sampling periods (March, June, August, and October) at the four sites that comprise the Substrate Age Gradient of Arizona. Data are means ± one standard error (n = 5)

Data analysis and statistical methods

To analyze the effect of season and substrate age across all four SAGA sites on unfertilized soil nutrient availability, the soil physical environment, and soil GHG fluxes, we used two-way repeated measures analysis of variance (RMANOVA). To analyze the effect of fertilization, substrate age, and season on soil nutrient availability, the soil physical environment, and soil GHG fluxes, we used three-way RMANOVA using data from the three oldest sites only. In both cases, we used RMANOVA to overcome violations of independence associated with autocorrelation between seasonal measurements. We expressed the effect of fertilization on soil nutrients, the soil physical environment, and soil GHG fluxes, as a relative effect size:

$$\frac{(Fertilized - Unfertilized)}{Unfertilized} \times 100\%.$$

We used two-tailed *t*-test to ascertain if soil nutrients, the soil physical environment, or soil GHG fluxes significantly differed between fertilized and unfertilized soil (if the effect size significantly differed from zero). Before performing RMANOVA and *t* test analyses, we took the natural log of soil NH_4^+, NO_3^-, total available N, available P, and WP (but not soil GHG fluxes, GWC, or temperature, which met statistical assumptions) to transform the data and meet statistical model assumptions of normality and homoscedasticity. However, only untransformed data are presented for clarity. For all parametric statistics, we set our alpha, a priori, at 0.10 because we were concerned of the possibility of Type II errors given our small sample size (n = 5) and anticipated large spatial and temporal variability in this study. To explore relationships between soil GHG fluxes, substrate age, season, soil nutrients, soil temperature, and soil water availability, we used regression tree analysis. Regression tree analysis is a machine learning recursive partitioning statistical approach that is robust for violations of assumptions of the true model, and allows for visual, simplified interpretation of the often complex multiple interactions between predictive and independent variables (De'ath and Fabricius 2000). We chose to use regression tree analysis rather than, for example, multiple or stepwise regression, because it represents the most important mechanistic variables related to soil GHG fluxes independently of a priori hypotheses that could bias our choice of initial model conditions (e.g., parabolic and linear relationships between temperature, water content, and soil CO_2 efflux; Sullivan et al. 2011). All statistical analyses were performed using open source R software (version 3.1.1; R Core Team 2014); regression tree analysis was performed using the "rpart" package in R (version 4.1–8; Therneau and Atkinson 2014).

Though substrate ages across the SAGA are unreplicated, the use of unreplicated substrate age gradients nonetheless provides important opportunities for the study of soil and ecosystem development and associated biogeochemical processes across long time scales (Vitousek 2002; Wardle et al. 2004). While

Table 2 Soil water potentials (MPa) in unfertilized soil from each of the four sites at the Substrate Age Gradient of Arizona during each sampling date

Substrate age	Sampling period			
(ky)	March	June	August	October
0.93	−0.01 (0.01)	−30.32 (5.99)	−0.00 (0.00)	−0.00 (0.00)
55	−0.29 (0.13)	−115.3 (18.0)	−0.01 (0.00)	−0.09 (0.01)
750	−0.72 (0.46)	−50.04 (10.8)	−1.78 (1.03)	−1.71 (1.49)
3000	−0.64 (0.47)	−41.09 (7.73)	−0.00 (0.00)	−0.00 (0.00)

Data are means ± one standard error (n = 5)

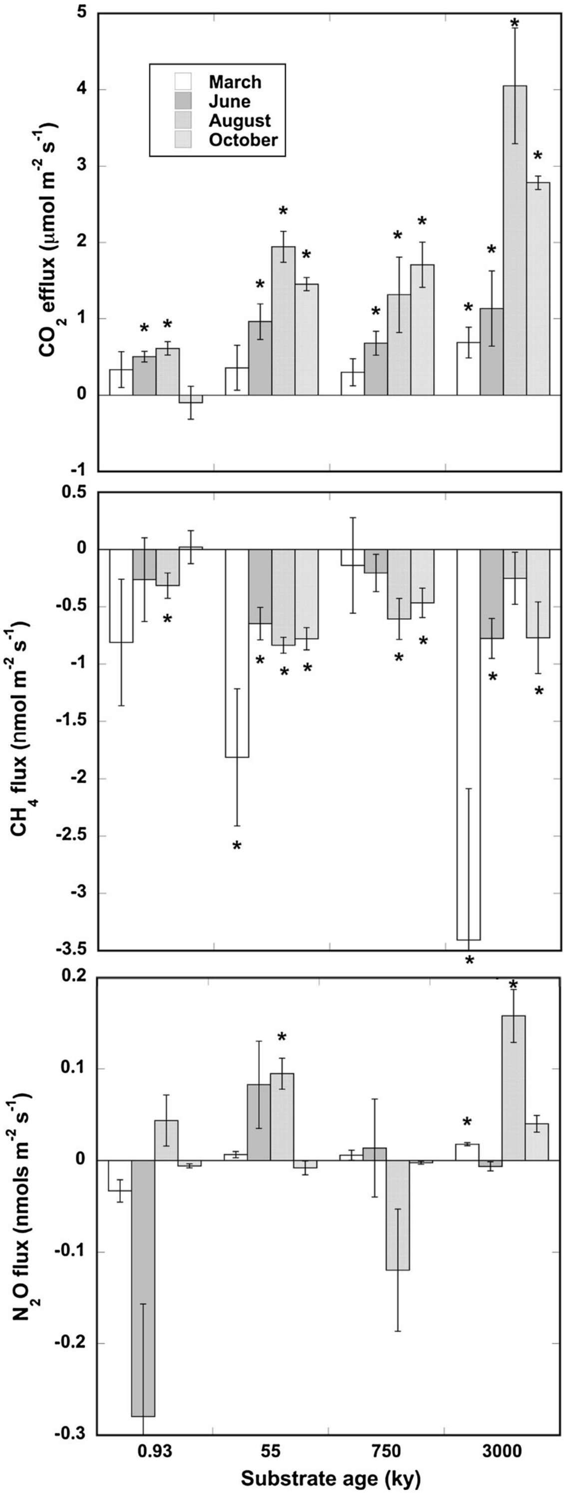

◀**Fig. 2** Soil carbon dioxide (CO_2; *top panel*), methane (CH_4; *middle panel*), and nitrous oxide (N_2O; *bottom panel*) measured during four sampling periods (March, June, August, and October) at the four sites that comprise the Substrate Age Gradient of Arizona. Data are means ± one standard error (n = 5). Positive values represent a net flux to the atmosphere and negative values represent a flux into the soil. *Asterisks* indicate the mean flux was significantly different from zero, measured using two-tailed *t*-test and $\alpha = 0.10$

some have questioned the utility of chronosequences (e.g., Johnson and Miyanishi 2008), such concerns often revolve around short- and medium-length chronosequences focused on vegetation succession. Rather, we focus on the effects of long-term soil development on clear, demonstrated soil physical and chemical characteristics—a "valid" use of chronosequences (Walker et al. 2010). Therefore, we proceeded to use parametric statistics to infer differences among sites, but the results and inferences herein should not be extrapolated to other sites without caution. All raw data associated with fluxes and soil properties, from each season, will be archived in the free online data repository Dryad (http://www.datadryad.org).

Results

Substrate age and seasonal effects on soil temperature, water content, nutrients, and GHG fluxes in unfertilized soil

Soil temperature at the 10 cm mineral soil depth in unfertilized plots varied significantly by season ($F_{(3,48)} = 569$, $p < 0.001$) but the seasonal trends depended on substrate age (season by substrate age interaction $F_{(9,48)} = 44.0$, $p < 0.001$; Fig. 1). At the three oldest sites, March was the coldest month, but at the youngest site, October was coldest. At all sites, June had the warmest soil temperature. Soil temperature did not vary significantly by substrate age alone ($F_{(3,16)} = 0.94$, $p = 0.446$).

Soil GWC in the top 10 cm mineral soil also varied significantly by season ($F_{(3,48)} = 51.0$, $p < 0.001$) and there was a significant interaction between season and substrate age ($F_{(9,48)} = 3.72$, $p = 0.001$). June was consistently the driest season and August was the wettest season at all sites except the 750 ky site (Fig. 1). Soil GWC varied significantly by substrate age ($F_{(3,16)} = 22.8$, $p < 0.001$); mean soil GWC across all seasons increased consistently from 0.07 kg kg^{-1} at the 0.93 ky site to 0.17 kg kg^{-1} at the 3000 ky site. Patterns of soil WP were generally

Table 3 The effect size of nitrogen (N), phosphorus (P), and nitrogen and phosphorus (N + P) fertilization, calculated as a percent relative to unfertilized soils, on soil nutrient concentrations at each of the three older sites at the Substrate Age Gradient of Arizona that received fertilization, during each sampling date

Nutrient concentration	Site age (ky)	Fertilization	Effect size (%) by month			
			March	June	August	October
NH_4^+	55	N	7254 (4749)	**802 (242)**	1127.5 (638)	**8709 (3130)**
		P	9.4 (19.3)	0.1 (8.5)	358 (214)	1361 (1136)
		N + P	50,349 (30975)	**1482 (613)**	3478 (1620)	**4282 (1289)**
	750	N	8025 (4884)	260 (193)	4245 (3577)	**855 (366)**
		P	85.8 (67.9)	149 (185)	72.1 (73.2)	298 (268)
		N + P	5665 (3849)	**568 (250)**	7408 (3911)	**4560 (2092)**
	3000	N	3169 (1711.4)	708 (456)	**552 (172)**	**329 (113)**
		P	29.2 (42.8)	10.2 (30.4)	−26.4 (25.3)	26.2 (26.0)
		N + P	**3759 (1689)**	455 (433)	**2732 (932)**	**1024 (378)**
NO_3^-	55	N	**159 (50.4)**	**305 (68.1)**	**76.2 (21.4)**	7254 (4749)
		P	5.1 (11.9)	30.0 (33.9)	18.5 (16.6)	9.4 (19.3)
		N + P	**164 (70.6)**	**258 (67.6)**	**131 (58.5)**	50349 (30976)
	750	N	471 (326)	**180 (36)**	1200 (876)	**8025 (4884)**
		P	356 (358)	77.2 (96.8)	40.6 (46.4)	85.8 (67.9)
		N + P	**250 (56.4)**	**316.9 (82.0)**	2251 (1290)	**5665 (3849)**
	3000	N	**227 (93.8)**	184 (128)	237 (148)	3169 (1711)
		P	37.6 (46.1)	−3.7 (20.4)	15.6 (52.4)	29.2 (42.8)
		N + P	**376 (107)**	**192 (85.3)**	**203 (71.0)**	3759 (1689)
PO_4^{3-}	55	N	**96.1 (43.9)**	**111 (44.3)**	1016 (847)	74.5 (46.1)
		P	**224 (62.4)**	**222 (53.4)**	5580 (4692)	**280 (71.0)**
		N + P	**286 (72.3)**	**214 (49.9)**	2774 (1887)	**342 (93.8)**
	750	N	16.9 (28.8)	9.5 (17.2)	31.8 (29.5)	−4.7 (26.4)
		P	**216 (66.9)**	**165 (51.1)**	277 (135)	136 (75.4)
		N + P	**198 (53.8)**	**254 (82.5)**	247 (120)	107 (87.7)
	3000	N	133 (68.7)	56.1 (50.1)	−8.9 (37.1)	17.7 (35.6)
		P	581 (324)	**198 (68.7)**	**367 (144)**	**312 (137)**
		N + P	684 (321)	**184 (31.2)**	**466 (103)**	**298 (94.8)**

Data are means ± one standard error (n = 5)

Bold numbers indicate the effect size was significantly different from zero, measured using two-tailed *t*-test and $\alpha = 0.10$. Positive effect sizes denote greater pools of ammonium (NH_4^+), nitrate (NO_3^-), or orthophosphate (PO_4^{3-}) in fertilized plots relative to unfertilized plots; negative effect sizes denote lower nutrient concentrations in fertilized than unfertilized plots

similar to GWC. Soil WP varied significantly by substrate age ($F_{(3,16)} = 29.18$, $p < 0.001$) and season ($F_{(3,48)} = 562$, $p < 0.001$), and there was a significant substrate age by season interaction ($F_{(9,48)} = 6.268$, $p < 0.001$; Table 2).

Soil nutrients always varied by season and generally varied by substrate age. Soil NH_4^+ ($F_{(3,48)} = 13.4$, $p < 0.001$), NO_3^- ($F_{(3,48)} = 2.84$, p = 0.048), available N ($F_{(3,48)} = 3.14$, $p = 0.034$), and available P ($F_{(3,48)} = 85.8$, $p < 0.001$) varied by season. Soil NO_3^- ($F_{(3,16)} = 10.9$, $p < 0.001$), available N ($F_{(3,16)} = 4.26$, $p = 0.022$), and available P ($F_{(3,16)} = 90.1$, $p < 0.001$) varied by substrate age. Any seasonal influence varied by substrate age for every soil nutrient we measured: Soil NH_4^+ ($F_{(9,48)} = 2.40$, $p = 0.025$), NO_3^- ($F_{(9,48)} = 3.03$, $p = 0.006$), available N ($F_{(9,48)} = 2.27$, $p = 0.033$), and available P concentrations ($F_{(9,48)} = 3.66$,

Table 4 The effect size of nitrogen (N), phosphorus (P), and nitrogen and phosphorus (N + P) fertilization, calculated as a percent relative to unfertilized soils, on soil greenhouse gas fluxes at each of the three older sites at the Substrate Age Gradient of Arizona that received fertilization, during each sampling date

Gas	Site age (ky)	Fertilization	Effect size (%) by month			
			March	June	August	October
CO_2 efflux	55	N	−71.4 (59.8)	−32.9 (13.8)	4.2 (6.9)	−46.7 (11.9)
		P	79.8 (35.5)	−916.3 (403.6)	−4.4 (8.5)	7.7 (4.9)
		N + P	−7.5 (70.6)	−86.3 (40.3)	**20.3 (3.6)**	125.6 (49.9)
	750	N	−50.1 (52.8)	−637.8 (167.3)	33.4 (13.7)	−17.3 (24.8)
		P	50.5 (19.5)	33.1 (7.0)	41.6 (12.4)	**31.3 (4.1)**
		N + P	22.4 (18.6)	96.6 (113.3)	43.4 (11.0)	−314.6 (142.7)
	3000	N	**35.4 (3.6)**	−10.4 (17.2)	−27.4 (10.2)	−49.2 (26.6)
		P	−0.9 (11.4)	**31.2 (3.7)**	−32.2 (13.1)	−7.7 (8.5)
		N + P	**14.9 (2.3)**	25.2 (7.8)	−38.2 (10.9)	5.3 (4.0)
CH_4 uptake	55	N	−9.7 (66.2)	161.5 (71.0)	−27.5 (9.6)	−18.6 (18.1)
		P	−160.2 (49.9)	31.5 (7.7)	**−79.9 (15.2)**	19.9 (5.8)
		N + P	267.2 (94.0)	**34.4 (4.9)**	−116.5 (29.2)	−15.4 (13.5)
	750	N	46.0 (40.5)	−28.0 (33.4)	2.4 (27.3)	42.9 (12.4)
		P	109.8 (34.0)	57.6 (10.9)	22.0 (11.5)	75.9 (16.9)
		N + P	−214.2 (156.9)	166.7 (43.8)	20.7 (10.8)	22.1 (35.7)
	3000	N	−47.8 (59.1)	−47.3 (17.4)	120.9 (81.4)	−217.1 (96.5)
		P	−164.2 (35.6)	−172.3 (84.1)	181.8 (81.1)	−78.0 (53.8)
		N + P	−47.9 (77.8)	6.4 (26.0)	184.2 (69.0)	−164.1 (36.0)
N_2O production	55	N	73.6 (16.6)	311.7 (95.8)	−30.4 (48.8)	**167.6 (20.1)**
		P	**140.7 (7.0)**	451.2 (159.1)	−173.1 (157.1)	321.7 (136.6)
		NP	115.6 (27.3)	212.8 (58.0)	148.4 (82.7)	69.6 (58.8)
	750	N	436.7 (202.5)	−7.3 (50.1)	−1052 (416.4)	91.2 (20.1)
		P	539.0 (237.0)	324.4 (126.8)	**739.0 (144.8)**	**133.6 (20.8)**
		NP	166.8 (39.2)	365.7 (86.3)	−1491 (471.4)	56.1 (22.2)
	3000	N	−141.8 (51.3)	**103.8 (20.1)**	**50.6 (10.6)**	**66.1 (7.6)**
		P	−162.5 (94.1)	**112.8 (10.8)**	−55.5 (36.1)	60.0 (18.6)
		NP	**103.1 (14.0)**	59.6 (26.8)	119.5 (27.5)	**84.2 (3.8)**

Data are means, ± one standard error (n = 5)

Bold numbers indicate the effect size was significantly different from zero, measured using two-tailed *t*-test and $\alpha = 0.10$. Positive effect sizes denote increased carbon dioxide (CO_2) efflux, methane (CH_4) uptake, and nitrous oxide (N_2O) production in fertilized plots relative to unfertilized plots; negative effect sizes denote less CO_2 efflux, CH_4 uptake (or CH_4 production), and N_2O production (or N_2O uptake) in fertilized plots relative to unfertilized plots

$p = 0.002$) had significant substrate age by season interactions (Fig. 1). There were few consistent patterns in soil available N; for example, concentrations were greatest in June at the 0.93 ky site, August at the 55 ky site, October at the 750 ky site, and March at the 3000 ky site (Fig. 1). Soil available P increased to a maximum between 0.93 and 750 ky (from 2.66 mg kg^{-1} at the 0.93 ky site to 57.7 mg kg^{-1} at the 750 ky site, averaged across all seasons) before declining at the 3000 ky site (Fig. 1). August consistently had the lowest available P concentrations at all sites, whereas October had the greatest available P concentration at the three oldest sites (Fig. 1).

In unfertilized soil, soil CO_2 efflux generally increased with increasing substrate age ($F_{(3,16)} = 12.1$, $p < 0.001$) and tended to increase during the growing season ($F_{(3,48)} = 28.3$, $p < 0.001$; Fig. 2). However, the seasonal effect varied by substrate age ($F_{(9,48)} = 7.17$, $p < 0.001$). At the 0.93, 55, and 3000 ky sites, soil CO_2 efflux declined at the end of the growing season (between August and October; Fig. 2).

As with soil CO_2 efflux, unfertilized soil CH_4 uptake varied significantly by substrate age ($F_{(3,16)} = 3.57$, $p = 0.038$), season ($F_{(3,48)} = 6.66$, $p < 0.001$), and exhibited a significant site by season interaction ($F_{(9,48)} = 2.77$, $p = 0.011$). Mean soil CH_4 uptake was greatest in March at the 0.93, 55, and 3000 ky sites (though not significantly different from zero at the 0.93 ky site, Fig. 2).

Unlike soil CO_2 efflux and CH_4 uptake, N_2O flux did not vary significantly by substrate age ($F_{(3,16)} = 1.96$, $p = 0.161$) or season ($F_{(3,48)} = 0.63$, $p = 0.599$), and there was no significant interaction between substrate age and season ($F_{(9,48)} = 1.01$, $p = 0.444$). Substantial within-site variability meant that most mean soil N_2O fluxes were not significantly different from zero, even when flux rates were substantial (Fig. 2). We only measured significant soil N_2O production in August at the 55 ky site and March and August at the 3000 ky site (Fig. 2).

Fertilization effects on nutrients, soil temperature, water content, and GHG fluxes

Fertilization significantly increased soil nutrient concentrations, but had no significant impacts on soil temperature, soil GWC, or WP. Nitrogen, but not P, fertilization significantly increased soil NH_4^+ concentrations ($F_{(3,48)} = 65.286$, $p < 0.001$). There was a significant interaction between fertilization treatment and season on soil NH_4^+ concentrations ($F_{(9,144)} = 2.162$, $p = 0.028$; Table 3). Soil NO_3^- concentrations were significantly higher in N, but not P, fertilized plots ($F_{(3,48)} = 37.9$, $p < 0.001$), and there were no significant interactions between fertilization or season or substrate age. The effect of N fertilization on soil NO_3^- was stronger in March and June than August and October (Table 3).

Soil available P concentrations were significantly different among fertilization treatments ($F_{(3,48)} = 31.2$, $p < 0.001$), and there were no significant interactive effects between fertilization treatment and substrate age and season on soil available P concentrations. Soil available P concentrations were consistently greater in P and N + P fertilized plots than in unfertilized plots, and like in N-fertilized plots, the fertilization effect was stronger in March and June than August and October (Table 3). Nitrogen fertilization significantly increased soil available P content

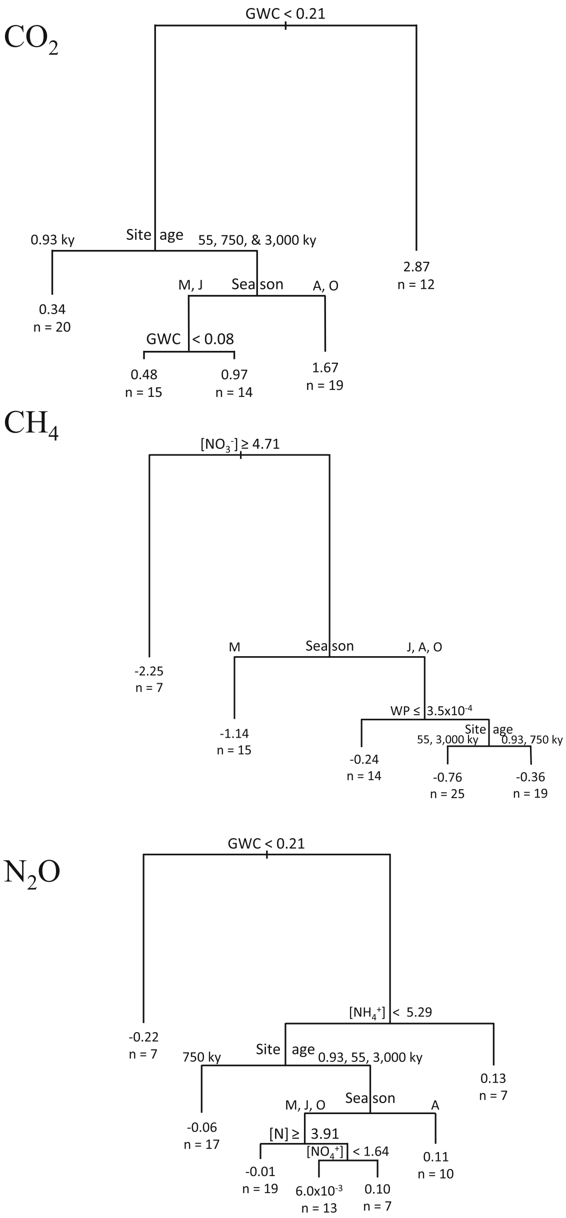

Fig. 3 Regression tree diagram depicting the interactive relationships between carbon dioxide (CO_2), methane (CH_4), and nitrous oxide (N_2O) in unfertilized soils only and numerous possible predictor variables. GWC: gravimetric water content, Site age: substrate age, NO_3^-: nitrate, WP: water potential, NH_4^+: ammonium, M: March, J: July, A: August, O: October, n: the number of fluxes measured at this terminal node. *Greater-than* or *less-than symbol*s (e.g., ≥, ≤ respectively) indicate a split at the node in which greater values are to the left or right indicated by the direction of the symbol

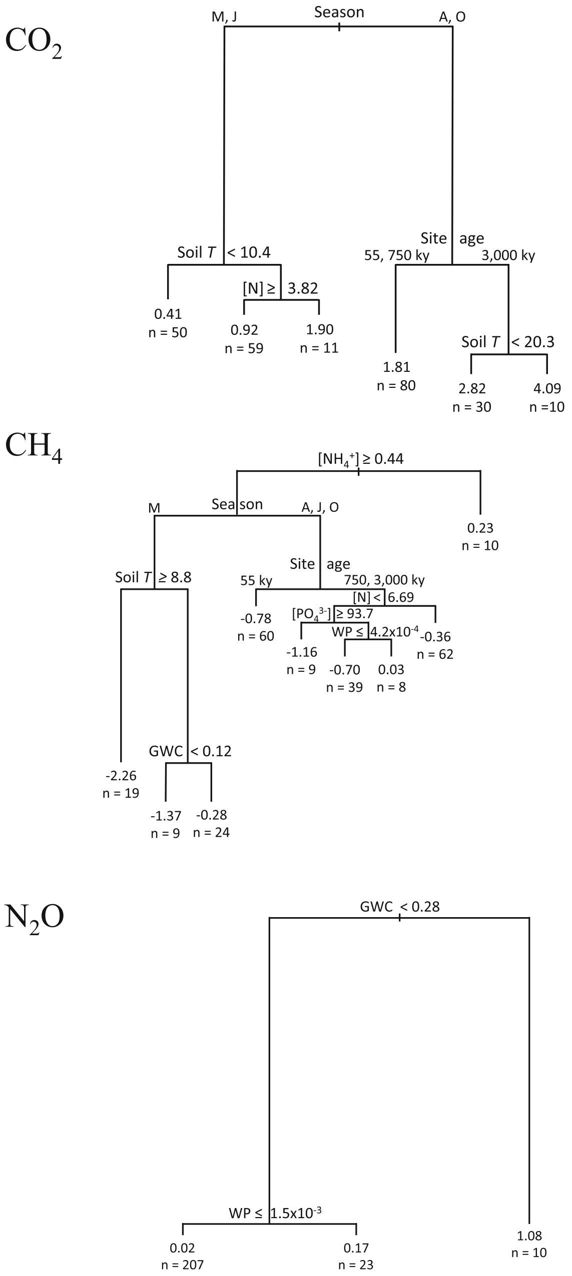

Fig. 4 Regression tree diagram depicting the interactive relationships between carbon dioxide (CO_2), methane (CH_4), and nitrous oxide (N_2O) in fertilized soils and numerous possible predictor variables. Soil T: soil temperature, N: soil available nitrogen, NH_4^+: ammonium, P: soil available P; GWC: gravimetric water content, Site age: substrate age, WP: water potential, M: March, J: July, A: August, O: October, n: the number of fluxes measured at this terminal node. *Greater-than* or *less-than symbols* (e.g., ≥, ≤ respectively) indicate a split at the node in which greater values are to the left or right indicated by the direction of the symbol

relative to unfertilized soils in March and June (but not August or October) at the 55 ky site (Table 3).

Seven years of fertilization had inconsistent effects on soil GHG fluxes. Soil CO_2 efflux did not vary significantly due to fertilization ($F_{(3,48)} = 0.41$, $p = 0.745$), nor were there any significant fertilizer interactions with substrate age ($F_{(6,48)} = 0.50$, $p = 0.806$), season ($F_{(9,144)} = 0.44$, $p = 0.913$), or substrate age and season ($F_{(18, 144)} = 0.816$, $p = 0.680$). Fertilization only significantly increased soil CO_2 efflux relative to unfertilized plots five times across all fertilization treatments, substrate ages, and seasons (36 possible combinations; Table 4).

Soil CH_4 uptake was even less responsive to fertilization than soil CO_2 efflux. However, while we found no overall fertilization effect ($F_{(3,48)} = 2.10$, $p = 0.117$), we did measure a significant fertilization by season interaction effect on soil CH_4 uptake ($F_{(9,44)} = 2.52$, $p = 0.010$). Fertilization significantly changed soil CH_4 uptake relative to unfertilized plots only twice; one effect was positive and the other was negative (Table 4). There were no significant fertilization by substrate age or substrate age by season by fertilization interactions on soil CH_4 uptake.

Soil N_2O fluxes were the more responsive to fertilization of the three GHGs measured, but, similar to the other GHGs, fertilization did not significantly affect N_2O flux overall ($F_{(3,48)} = 1.44$, $p = 0.244$). We did not find significant interactions between fertilization, substrate age, and season. However, fertilization increased mean soil N_2O flux in 10 out of 36 possible fertilization, season, and substrate age combinations (Table 4). The most consistent fertilization impact on soil N_2O flux was an increase in soil N_2O production in June, August, and October at the 3000 ky site in N fertilized plots relative to control sites (Table 4). Although soil N_2O production was greater on P fertilized plots than unfertilized plots in one-third of the cases, responses were inconsistent among all sites and seasons (Table 4).

Chamber-scale controls on GHG fluxes

As measured by regression tree analysis, the dominant controls of unfertilized soil CO_2 efflux were soil GWC, substrate age, and season, in descending order of importance (Fig. 3). Soil CO_2 efflux was greatest in moist soils. However, the dominant controls on fertilized soil CO_2 efflux were, in order, season, soil temperature, substrate age, and total soil available N concentration (Fig. 4). Soil CO_2 efflux in fertilized plots split into low rates in March and June and higher rates in August and October.

Soil NO_3^- concentration, season, WP, and site age were the dominant controls on unfertilized soil CH_4 uptake, in descending order of importance (Fig. 3). Soil CH_4 uptake was greatest when soil NO_3^- concentrations were lower than 4.71 mg kg^{-1}; in March, when soil NO_3^- exceeded that threshold, CH_4 uptake was greater than any of the other months. There were more factors that controlled soil CH_4 uptake in fertilized plots than unfertilized plots. Soil NH_4^+ concentration, season, soil temperature, site age, total soil available N, soil available P concentration, WP, and GWC were all factors that demarcated branches of our regression tree (Fig. 4). Soil CH_4 uptake was lowest when soil NH_4^+ concentrations were greater than 0.44 mg kg^{-1}.

The dominant controls of unfertilized soil N_2O flux were GWC, soil NH_4^+ concentration, site age, season, soil available N concentration, and soil NO_3^- concentration, in descending order of importance (Fig. 3). Soil N_2O uptake occurred with soil GWC below 0.21 kg kg^{-1}, whereas soil N_2O production predominated when soil GWC exceeded that threshold. By contrast, the regression tree analysis only identified two controls on fertilized soil N_2O production: GWC and WP (Fig. 4).

Discussion

Our results indicate that the mechanisms that control soil GHG fluxes in these semiarid soils are similar to those in more humid ecosystems, with some important distinctions. Nutrient fertilization appears to alter the mechanistic controls over soil GHG fluxes in semiarid soils.

Unfertilized soils

We expected soil CO_2 efflux rates to be driven by a combination of seasonal climate dynamics and soil nutrient availability. Therefore, we correctly anticipated that soil CO_2 efflux would be greatest during the August sampling dates, which had warm and wet conditions (brought on by the late-summer "monsoonal" precipitation pattern that dominates the southwestern U.S. climate; Sheppard et al. 2002). Yet, among the SAGA sites, we expected soil CO_2 efflux to reflect the retrogressive pattern of C and N pools and fluxes that has been repeatedly demonstrated among these sites (Table 1; Selmants and Hart 2008; Sullivan et al. 2012; Looney et al. 2012; Newman and Hart 2015). The retrogressive decline in C and N availability between the 750 and 3000 ky sites has been ascribed to P limitation (Peltzer et al. 2010) brought on by a decline in plant and microbially available P pools (Selmants and Hart 2010). Therefore, we were surprised to measure higher rates of soil CO_2 efflux at the 3000 ky than the 750 ky site in every season. Though it would seem that both C supply and nutrients were optimal for heterotrophic and autotrophic soil CO_2 efflux at the 750 ky site, the 3000 ky site had the finest-textured soil of the SAGA sites. The higher silt and clay content of this soil allows for greater water holding capacity than the other sites (Selmants and Hart 2008, Sullivan et al. 2013). Our regression tree analysis suggested that the highest rates of soil CO_2 efflux in unfertilized soil occurred in wetter soils. While each site, on average, receives similar precipitation, the finer-textured soil at the 3000 ky site likely led to the two highest water contents we measured (in August and October, Fig. 1) when soil CO_2 efflux was also highest (Fig. 2). These results suggest that soil CO_2 efflux is more limited by water availability than C availability, nutrient availability, or temperature among these semiarid sites. Further, the trend of increasing soil CO_2 efflux with increasing substrate age (and water holding capacity) is consistent with more humid ecosystems where soil CO_2 efflux increases linearly with soil water availability (Raich and Schlesinger 1992).

In both humid and arid ecosystems, soil water availability is an important driver of soil CH_4 uptake. Low soil water content can limit CH_4 uptake (Striegl et al. 1992). For example, models of CH_4 uptake predict a sharp decline below 5–10 % GWC, depending on the soil texture (Del Grosso et al. 2000). By contrast, too much soil water reduces the air-filled pore space through which soil gas diffuses, and therefore can inhibit atmospheric CH_4 diffusion into soil (Striegl 1993). The patterns and proximate controls of soil CH_4 uptake we observed were at least partially contrary to our expectations. First, in three of four sites, the highest rate of soil CH_4 uptake occurred in March, when temperatures were cold and water contents were intermediate. Second, the regression tree analysis provided little evidence that either soil water content or soil temperature were strong controls on soil CH_4 uptake. We measured significant rates of soil CH_4 uptake in both dry soil (e.g., June at the 55 ky site) and wet soil (e.g., October at the 3000 ky site). Furthermore, soil NO_3^- concentration was the first-order control of soil CH_4 uptake. While NO_3^- fertilizer has been shown to reduce soil CH_4 uptake and soil CH_4 uptake has been negatively correlated with nitrification rates (Aronson and Helliker 2010; Neff et al. 1994), the mechanism behind the relationship between soil CH_4 uptake and soil NO_3^- concentration is not well understood, especially in arid soils.

We measured a wide range of soil N_2O production and consumption that reflected the wide range of soil water content and N availability among sites and seasons. Though we only measured three instances of significant N_2O production, in part because of the spatial and temporal variability of the process, two of those instances occurred at the 3000 ky site. Selmants and Hart (2008) measured greater soil ^{15}N enrichment (~ 7 ‰) at this site than any of the other SAGA sites, and hypothesized that this was due to the fractionating effects of nitrification and denitrification at a site that was N-rich and P-poor. While similar hypotheses have been robust at other age gradients in humid ecosystems (e.g., Martinelli et al. 1999), our data provide limited evidence for greater rates of gaseous N losses late in primary succession in semiarid environments. It also appears that N_2O production is almost entirely dependent on soil water content and N availability (Fig. 3). In most cases, the regression tree analysis showed that soil N_2O production increased as GWC and soil N availability increased.

Fertilized soil

Seven years of annual N, P, and N + P fertilization at the three oldest SAGA sites had substantial effects on soil nutrient availability, but surprisingly few effects on soil GHG fluxes. Our results suggest that our experimental design was largely successful for two reasons. First, there was very little cross-plot movement of fertilizer (Table 3). Second, annual fertilizer additions raise the possibility that impacts on transient processes like soil GHG fluxes would only be observed immediately after fertilization (Sullivan et al. 2014). However, in this case, 7 years of fertilization appear to have caused persistent increases in soil nutrients, even in June, 11 months after the last fertilizer application. In fact, the sampling date with the least number of significant fertilization effects on soil nutrients was August, only 1 month after fertilization. This seemingly paradoxical result is likely due to plant utilization of fertilizer being greatest during the August growing season, when monsoonal rains and warm temperatures are ideal for plant growth; during our October sampling period, soil nutrients were again significantly greater in fertilized plots than unfertilized plots after grass aboveground senescence in late September. Nevertheless, our data raise the question: by what mechanism do the grasses release the nutrients, derived initially from fertilizer uptake, back into available soil pools after the growing season?

Fertilizer addition had surprisingly few significant impacts on soil CO_2 efflux and CH_4 uptake. There was no evidence that fertilizer alleviated nutrient constraints on soil CO_2 efflux in a manner consistent with biogeochemical theory. Based on the retrogressive nutrient patterns demonstrated among the SAGA sites by Selmants and Hart (2008, 2010), and the response of grass primary production to 1 year of fertilization (Newman and Hart 2015), we were surprised that N fertilization did not increase soil CO_2 efflux at the 55 ky site and P fertilization did not increase soil CO_2 efflux at the 3000 ky site (Table 4). Like in this study, N and P fertilization across a retrogressive, tropical montane chronosequence had only muted effects on litter decomposition (an important source of CO_2 efflux) across 4100 ky of soil development despite responses of aboveground productivity (Vitousek and Farrington 1997; Hobbie and Vitousek 2000). Soil temperature and water content exhibited stronger controls on soil CO_2 efflux than nutrient availability in these semiarid soils.

In fertilized soils, NH_4^+ availability appeared to be the first-order control over CH_4 uptake; soil CH_4 uptake declined with increasing NH_4^+ availability. Relationships between inorganic N and soil CH_4 uptake have been previously documented in more humid ecosystems. For instance, the suppressive effects of N addition on soil CH_4 uptake increase with increasing duration of fertilization (Aronson and Helliker 2010), but arid ecosystems were underrepresented in that analysis. Here, we observed two different N influences on CH_4 uptake. Across naturally occurring gradients of N availability in unfertilized soil, soil CH_4 uptake appeared to increase with increasing NO_3^- availability, whereas among fertilized plots, NH_4^+ suppressed CH_4 uptake. In both cases, N availability was a more proximate control of soil CH_4 uptake than either soil water content or soil texture. These patterns point to complex, poorly understood mechanisms that control soil CH_4 uptake in semiarid ecosystems (Sullivan et al. 2013).

Based simply on the number of significant effect sizes, fertilization had a greater effect on soil N_2O production than the other two GHG fluxes. Given that N availability must be sufficient for nitrification and denitrification, the two dominant sources of N_2O production in soil (Davidson et al. 1986), we expected N and N + P fertilization to increase N_2O production. However, we found an equal number of cases (four) with significant positive P effects on N_2O production as N effects, and a surprising number (four) of non-significant *negative* N fertilization effects on N_2O production (Table 4). While meta-analysis has demonstrated that N additions nearly always resulted in an increase in N_2O production (Aronson and Allison 2012), semiarid and arid ecosystems were underrepresented, as they were for soil CH_4 fluxes. At present, any link between P fertilization and N_2O production is uncertain. For example, a synthesis highlighting the need for denitrification studies does not mention the role of P in denitrification (Davidson and Seitzinger 2006). The simplest explanation of these results may be that, in some conditions, P fertilization alleviated plant or microbial limitation and increased biological activity and N cycling. Regardless, fertilization removed N constraints on N_2O production. While N_2O fluxes in unfertilized soils indicated appeared to be controlled by N and water availability, fertilized soils were only controlled by water availability (Fig. 4). Aside from the unknown mechanism that caused P fertilization to increase N_2O fluxes 25 % of the time, N_2O production in both humid and arid ecosystems, whether from nitrification or denitrification, seems to depend on both soil N availability and water.

Conclusions

A paucity of data and a corresponding lack of a mechanistic understanding of soil GHG fluxes in arid environments have hindered consideration of these environments in many global biogeochemical models, despite their spatial extent. Substrate age gradients, combined with long-term fertilizations, can provide valuable information about limitation of ecosystem processes because they seek to constrain many state factors while allowing nutrients and soil physical properties to change over time with soil development (Vitousek 2004; Sullivan et al. 2014). By using a long-term in situ nutrient manipulation experiment at the SAGA to explore interactions between pedogenesis, soil physics, biogeochemistry, and soil GHG fluxes, our results highlight important controls on soil GHG fluxes in semiarid soils and raise several questions. Our results demonstrate that the mechanistic understanding of soil GHG fluxes derived in humid ecosystems does not apply consistently to the three GHG fluxes we measured here. We suggest that the applicability of mechanisms that drive GHG fluxes in humid ecosystems to semiarid ecosystems declines in the following order: $N_2O > CO_2 > CH_4$. Clearly, N and water availability controlled unfertilized soil N_2O fluxes (and fertilization reduced N limitation of N_2O flux). However, we are unable to adequately explain relationships between soil N availability and soil CH_4 flux, and we note the lack of apparent relationships between soil CH_4 uptake and soil physical properties. By combining in situ observation with experimentation and regression tree analysis, our results have elucidated the separate and complex controls on soil GHG fluxes in semiarid soils that we hope will lead to development of better mechanistic models of soil GHG fluxes in arid climates.

Acknowledgments This research was supported by a Hooper Undergraduate Research Award and funding from the Ecological Restoration Institute at NAU to M.K.N., a Mission Research Program grant to B.W.S. and S.C.H., and an NSF IGERT fellowship to B.W.S. We thank S.R. Jackson for her assistance in the lab and field, and S. Alvarez Clare and several anonymous reviewers for helpful comments on this manuscript. We especially appreciate the efforts of G.S. Newman and K.L. Hess in establishing the fertilization plots across the SAGA.

References

Aronson EL, Allison SD (2012) Meta-Analysis of environmental impacts on nitrous oxide release in response to N amendment. Front Microb 3:272

Aronson EL, Helliker BR (2010) Methane flux in non-wetland soils in response to nitrogen addition: a meta-analysis. Ecology 91:3242–3251

Austin AT (2011) Has water limited our imagination for aridland biogeochemistry? Trends Ecol Evol 26(5):229–235

Austin AT, Yahdjian L, Stark JM, Belnap J, Porporato A, Norton U, Ravetta DA, Schaeffer SM (2004) Water pulses and biogeochemical cycles in arid and semiarid ecosystems. Oecologia 141(2):221–235

Bremner JM (1997) Sources of nitrous oxide in soils. Nutr Cycling Agroecosyst 49:7–16

Chapuis-Lardy L, Wrage N, Metay A, Chotte J, Bernoux M (2007) Soils, a sink for N_2O? A review. Glob Change Biol 13:1–17

Ciais P, Sabine C, Bala G, Bopp L, Brovkin V, Canadell J, Chhabra A, DeFries R, Galloway J, Heimann M, Jones C, Le Quéré C, Myneni RB, Piao S, Thornton P (2013) Carbon and other biogeochemical cycles. In: Stocker TF, Qin D, Plattner GK, Tignor M, Allen SK, Boschung J, Nauels A, Xia Y, Bex V, Midgley PM (eds) Climate Change 2013: The Physical Science Basis. Contribution of Working Group 1 to the Fifth Assessment Report of the Intergovernmental Panel on Climate Change. Cambridge University Press, New York

Cleveland CC, Townsend AR (2006) Nitrogen and phosphorus additions cause substantial losses of soil carbon from a lowland tropical rain forest. Proc Natl Acad Sci USA 103:10316–10321

Crutzen PT (1974) Estimates of possible variations in total ozone due to natural causes and human activities. Ambio 3(6):201–210

Davidson EA, Seitzinger S (2006) The enigma of progress in denitrification research. Ecol Appl 16:2057–2063

Davidson EA, Swank WT, Perry TO (1986) Distinguishing between nitrification and denitrification as sources of gaseous nitrogen production in soil. Appl Environ Microbiol 52(6):1280–1286

De'ath G, Fabricius KE (2000) Classification and regression trees: A powerful yet simple technique for ecological data analysis. Ecology 81:3178–3192

Del Grosso SJ, Parton WJ, Mosier AR, Ojima DS, Potter CS, Borken W, Brumme R, Butterbach-Bahl K, Crill PM, Dobbie K, Smith KA (2000) General CH4 oxidation model and comparisons of CH4 oxidation in natural and managed systems. Global Biogeochem Cy 14(4):999–1019

Dutaur L, Verchot L (2007) A global inventory of the soil CH4 sink. Global Biogeochem Cy 21:GB4013

Elser JJ, Bracken MES, Cleland EE, Gruner DS, Harpole WS, Hillebrand H, Ngai JT, Seabloom EW, Shurin JB, Smith JE (2007) Global analysis of nitrogen and phosphorus limitation of primary producers in freshwater, marine and terrestrial ecosystems. Ecol Lett 10:1135–1142

Galbally I, Meyer CP, Wang Y-P, Kirstine W (2010) Soil-atmosphere exchange of CH_4, CO, N_2O, and NO_x and the effects of land-use change in the semiarid Mallee system in Southeastern Australia. Glob Chang Biol 16:2407–2419

Hashimoto S, Carvalhais N, Ito A, Migliavacca M, Nishina K, Reichstein M (2015) Global spatiotemporal distribution of soil respiration modeled using a global database. Biogeosciences Discuss 12:4331–4364

Hobbie S, Vitousek P (2000) Nutrient limitation of decomposition in Hawaiian forests. Ecology 81(7):1867–1877

Houghton JT, Meira Filho LG, Callander BA, Harris N, Kattenberg A, Maskell K (1996) Climate change 1995: The science of climate change. Cambridge University Press, Cambridge

Jenny H (1941) Factors of soil formation. McGraw-Hill, New York

Johnson EA, Miyanishi K (2008) Testing the assumptions of chronosequences in succession. Ecol Lett 11:419–431

Lal R (2004) Carbon sequestration in dryland ecosystems. Environ Manage 33(4):528–544

Le Mer J, Roger P (2001) Production, oxidation, emission and consumption of methane by soils: a review. Eur J Soil Biol 37:25–50

Looney CE, Sullivan BW, Kolb TE, Kane JM, Hart SC (2012) Pinyon pine (*Pinus edulis*) mortality and response to water addition across a three million year substrate age gradient in northern Arizona, USA. Plant Soil 357:89–102

Mahecha MD, Reichstein M, Carvalhais N, Lasslop G, Lange H, Seneviratne SI, Vargas R, Ammann C, Arain MA, Cescatti A, Janssens IA, Migliavacca M, Montagnani L, Richardson AD (2010) Global convergence in the temperature sensitivity of respiration at ecosystem level. Science 329:838–840

Martin LJ, Blossey B, Ellis E (2012) Mapping where ecologists work: biases in the global distribution of terrestrial ecological observations. Front Ecol Environ 10(4):195–201

Martinelli LA, Piccolo MC, Townsend AR, Vitousek PM, Cuevas E, McDowell W, Robertson GP, Santos OC, Treseder K (1999) Nitrogen stable isotopic composition of leaves and soil: tropical versus temperate forests. Biogeochemistry 46:45–65

Montzka SA, Dlugokencky EJ, Butler JH (2011) Non-CO_2 greenhouse gases and climate change. Nature 476:43–50

Moore RB, Wolfe EW (1987) Geologic map of the east part of the San Francisco Volcanic Field, north-central Arizona, scale 1:50,000. Misc Field Stud Map MF-1960 US Geol Surv, Washington, DC

Neff JC, Bowman WD, Holland EA, Fisk MC, Schmidt SK (1994) Fluxes of nitrous oxide and methane from nitrogen-amended soils in a Colorado alpine ecosystem. Biogeochemistry 27(1):23–33

Neff JC, Townsend AR, Gleixner G, Lehman SJ, Turnbull J, Bowman WD (2002) Variable effects of nitrogen additions on the stability and turnover of soil carbon. Nature 419:915–917

Newman GS, Hart SC (2015) Shifting soil resource limitations and ecosystem retrogression across a three million year semi-arid substrate age gradient. Biogeochemistry 124(1–3):177–186

Nömmik H (1956) Investigations on denitrification in soil. Acta Agr Scand 6(2):195–228

Orchard VA, Cook FJ (1983) Relationship between soil respiration and soil moisture. Soil Biol Biochem 15(4):447–453

Parker SS, Schimel JP (2011) Soil nitrogen availability and transformations differ between the summer and the growing season in a California grassland. Appl Soil Ecol 48:185–192

Parton W, Silver WL, Burke IC, Grassens L, Harmon ME, Currie WS, King JY, Adair EC, Brandt LA, Hart SC, Fasth B (2007) Global-scale similarities in nitrogen release patterns during long-term decomposition. Science 315(5810):361–364

Peltzer DA, Wardle DA, Allison VJ, Baisden WT, Bardgett RD, Chadwick OA, Condron LM, Parfitt RL, Porder S, Richardson SJ, Turner BL, Vitousek PM, Walker J, Walker LR (2010) Understanding ecosystem retrogression. Ecol Monogr 80:509–529

Potter CS, Davidson EA, Verchot LV (1996) Estimation of global biogeochemical controls and seasonality in soil methane consumption. Chemosphere 32(11):2219–2246

Priest SS, Duffielt WA, Malis-Clark K, Hendley II JW, Stauffer PH (2001) The San Francisco Volcanic Field, Arizona. Fact Sheet 017-01. US Geol Surv, Washington D.C

R Core Team (2014) R: A language and environment for statistical computing. R Foundation for Statistical Computing, Vienna URL: http://www.R-project.org/

Raich JW, Schlesinger WH (1992) The global carbon dioxide flux in soil respiration and its relationship to vegetation and climate. Tellus B 44:81–99

Reynolds JF (2001) Desertification. In: Levin SA (ed) Encyclopedia of Biodiversity. Academic Press, San Diego

Running SW, Nemani RR, Heinsch FA, Zhao M, Reeves M, Hashimoto H (2004) A continuous satellite-derived measure of global terrestrial primary production. Bioscience 54(6):547–560

Safriel U, Adeel Z (2008) Development paths of drylands: thresholds and sustainability. Sustain Sci 3:117–123

Segers R (1998) Methane production and methane consumption: a review of processes underlying wetland methane fluxes. Biogeochem 41:23–51

Selmants PC (2007) Carbon, Nitrogen, and phosphorus dynamics across a three million year substrate age gradient in northern Arizona, USA. Ph.D. Thesis, Northern Arizona University

Selmants PC, Hart SC (2008) Substrate age and tree islands influence carbon and nitrogen dynamics across a retrogressive semiarid chronosequence. Glob Biogeochem Cycles 22:GB1021

Selmants PC, Hart SC (2010) Phosphorus and soil development: does the Walker and Syers model apply to semiarid ecosystems? Ecology 91(2):474–484

Sheppard PR, Comrie AC, Packin GD, Angersbach K, Hughes MK (2002) The climate of the US southwest. Clim Res 21(3):219–238

Shine KP, Sturges WT (2007) CO_2 is not the only gas. Science 315:1804–1805

Stark JM, Firestone M (1995) Mechanims for soil moisture effects on nitrifying bacteria. Appl Environ Microb 61(1):218–221

Striegl RG (1993) Diffusional limits to the consumption of atmospheric methane by soils. Chemosphere 26:715–720

Striegl RG, McConnaughey TA, Thorstenson DC, Weeks EP, Woodward JC (1992) Consumption of atmospheric methane by desert soils. Nature 357:145–147

Sullivan BW, Kolb TE, Hart SC, Kaye JP, Hungate BA, Dore S, Montes-Helu M (2011) Wildfire reduces carbon dioxide efflux and increases methane uptake in ponderosa pine forest soils of the southwestern USA. Biogeochemistry 104:251–265

Sullivan BW, Selmants PC, Hart SC (2012) New evidence that high potential nitrification rates occur in soils during dry seasons: are microbial communities metabolically active during dry seasons? Soil Biol Biochem 53:28–31

Sullivan BW, Selmants PC, Hart SC (2013) Does dissolved organic carbon regulate biological methane oxidation in semiarid soils? Glob Change Biol 19(7):2149–2157

Sullivan BW, Alvarez-Clare S, Castle SC, Porder S, Reed SC, Schreeg L, Townsend AR, Cleveland CC (2014) Assessing nutrient limitation in complex forested ecosystems: alternatives to large-scale fertilization experiments. Ecology 95(3):668–681

Tanaka K, Shoemaker EM, Ulrich GE, Wolfe TW (1986) Migration of volcanism in the San Francisco Volcanic Field, Arizona. Geol Soc Am Bull 97:129–141

Therneau T, Atkinson B (2014) An introduction to recursive partitioning using the RPART Routines. http://cran.r-project.org/web/packages/rpart/vignettes/longintro.pdf 62 pp

Vitousek PM (2002) Oceanic islands as model systems for ecological studies. J Biogeogr 29:573–582

Vitousek PM (2004) Nutrient cycling and limitation: Hawai'i as a model system. Princeton University Press, NJ

Vitousek PM, Farrington H (1997) Nutrient limitation and soil development: experimental test of a biogeochemical theory. Biogeochemistry 37:63–75

Vitousek PM, Howarth RW (1991) Nitrogen limitation on land and in the sea: How can it occur? Biogeochemistry 13:87–115

Walker TW, Syers JK (1976) The fate of phosphorus during pedogenesis. Geoderma 15:1–19

Walker LR, Wardle DA, Bardgett RD, Clarkson BD (2010) The use of chronosequences in studies of ecological succession and soil development. J Ecol 98:725–736

Wardle DA, Walker LR, Bardgett RD (2004) Ecosystem properties and forest decline in contrasting long-term chronosequences. Science 305:509–513

Webster EA, Hopkins DW (1996) Contributions from different microbial processes to N_2O emission from soil under different moisture regimes. Biol Fertil Soils 22:331–335